Inorganic Chemistry

Article

pubs.acs.org/IC

Synthesis and Charge-Transfer Dynamics in a Ferrocene-Containing Organoboryl aza-BODIPY Donor–Acceptor Triad with Boron as the Hub

Eranda Maligaspe,[†,‡] Tom J. Pundsack,[‡,§] Lauren M. Albert,[§] Yuriy V. Zatsikha,[†] Pavlo V. Solntsev,[†,§] David A. Blank,*[,§] and Victor N. Nemykin*[,†]

[†]Department of Chemistry and Biochemistry, University of Minnesota—Duluth, 1039 University Drive, Duluth, Minnesota 55812, United States

[§]Department of Chemistry, University of Minnesota, 207 Pleasant Street SE, Minneapolis, Minnesota 55455, United States

Supporting Information

ABSTRACT: A *N*,*N*′-bis(ferroceneacetylene)boryl complex of 3,3′-diphenylazadiisoindolylmethene was synthesized by the reaction of an *N*,*N*′-difluoroboryl complex of 3,3′-diphenylazadiisoindolylmethene and ferroceneacetylene magnesium bromide. The novel diiron complex was characterized by a variety of spectroscopic techniques, electrochemistry, and ultrafast time-resolved methods. Spectroscopy and redox behavior was correlated with the density functional theory (DFT) and time-dependent DFT calculations. An unexpected degree of coupling between the two Fc ligands was observed. Despite a lack of conjugation between the donor and acceptor, the complex undergoes very rapid (τ = 1.7 ± 0.1 ps) photoinduced intramolecular charge separation followed by subpicosecond charge recombination to form a triplet state with a lifetime of 4.8 ± 0.1 μs.

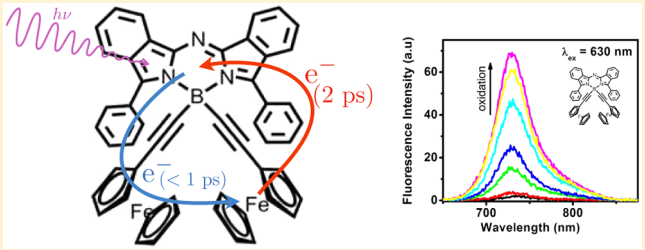

INTRODUCTION

The preparation of highly efficient functional materials for solar energy conversion is of fundamental interest.[1−5] Because of their outstanding absorption properties, numerous porphyrinoids coupled with organic or organometallic donor fragment(s) have been investigated in dye-sensitized solar cells and organic photovoltaics.[6−11] The photophysical properties of ferrocenylporphyrins, phthalocyanines, tetraazaporphyrins, and subphthalocyanines have recently been investigated by several research groups, and the ferrocene (Fc)-based substituents were found to be prominent electron-donating groups.[12−33] BODIPYs and aza-BODIPYs (where BODIPY = dipyrromethene boron difluoride) have recently emerged in this field because of their unique photophysical properties.[34−45] Several Fc-containing BODIPY conjugates with a Fc group linked via a spacer located at the α- or β-pyrrolic or meso position have been reported.[46−52] However, to the best of our knowledge, no reports are available on BODIPYs and aza-BODIPYs with Fc substituents connected via the central boron atom using direct organometallic B–C bonds. Bonding the Fc ligands at the boron atom leaves them in close proximity to aza-BODIPY but without conjugated through-bond coupling. This work was motivated by the potential to exploit a new balance between the donor–acceptor coupling for the enhancement of excited-state characteristics favorable for optoelectronic applications, for example, attempting to maintain efficient intramolecular charge separation with the inhibition of subsequent charge recombination. Suppression of through-bond coupling was also intended to allow characterization of through-space coupling between the two Fc moieties. The resulting molecular electronic states present more isolation between the donor and acceptor. However, the proximity and energetic alignment of charge-transfer and triplet excited states results in an unexpected, very rapid charge recombination to form a long-lived triplet excited state with very high efficiency.

Herein we report the preparation and characterization of the first organoboryl aza-BODIPY donor–acceptor triad **3** (Scheme 1) with B(C≡CFc)$_2$ fragments. Electronic coupling between the two Fc ligands is observed despite the relatively large separation distance. Direct binding of the electron donor to the acceptor at the boron atom results in photoinitiated charge transfer in <2 picoseconds (ps) even in the absence of conjugation between the donor and acceptor. Subsequent charge recombination takes place even faster. The result is efficient access to the triplet state mediated by charge transfer, which extends the excited-state lifetime by 3 orders of magnitude without the need for heavy atoms to enhance spin–orbit coupling.

Received: March 3, 2015
Published: March 30, 2015

ACS Publications © 2015 American Chemical Society

DOI: 10.1021/acs.inorgchem.5b00494
Inorg. Chem. 2015, 54, 4167−4174

Scheme 1. Preparation of the Target aza-BODIPYs

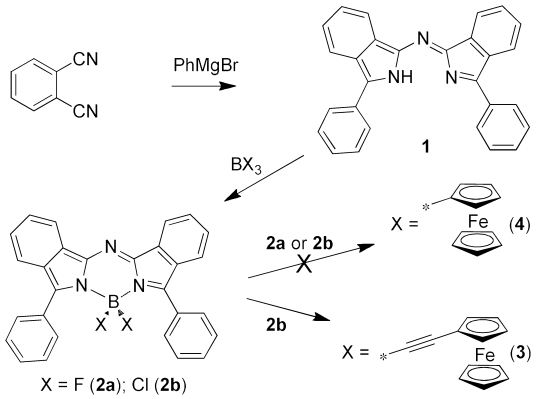

EXPERIMENTAL METHODS

Reagents and Materials. All reactions were performed under an argon atmosphere using standard Schlenk techniques. Solvents were purified by standard methods: tetrahydrofuran (THF) was distilled over a sodium–potassium alloy, toluene and diethyl ether were distilled over sodium metal, dichloromethane (DCM) and hexanes were distilled over calcium hydride under reduced pressure, and methanol was distilled over magnesium under an argon atmosphere. Bromobenzene, magnesium, NH_4Cl, diisopropylethylamine, $BF_3{\cdot}OEt_2$, a BCl_3 solution in hexanes, ethylmagnesium bromide, and ethynylferrocene were purchased from Aldrich and used without further purification. 1,2-Dicyanobenzene was purchased from Acros Organics and used without further purification. Silica gel (60 Å, 60–100 μm) was purchased from Dynamic Adsorbents Inc. Neutral alumina (50–200 μm) was purchased from Sorbent Technologies. Tetrabutylammonium tetrakis(pentafluorophenyl)borate (TBAF) was used in anhydrous DCM for electrochemical studies, after preparation according to literature procedures.[53,54]

Synthesis of *N*-(3-Phenyl-2*H*-isoindol-1-yl)-*N*-(3-phenyl-1*H*-isoindol-1-ylidene)amine (1). Compound **1** was prepared using a slightly modified procedure that was reported previously.[39] The Grignard reagent of phenylmagnesium bromide was prepared from 2.0 g (83 mmol) of magnesium in dry ether (5 mL) and 8.5 mL of bromobenzene at 0 °C (magnesium was activated by placing a small crystal of iodine in the flask and heated to observe a violet color). The resulting mixture was stirred for a further 1.5 h. The solution of phenylmagneisum bromide was added via cannula to a vigorously stirred dry toluene solution (30 mL) of 1,2-dicyanobenzene (4.25 g, 33.2 mmol) at 0 °C. After 2 h of stirring, 10 mL of a saturated ammonium chloride solution was slowly added to the resulting mixture. An additional 10 mL of water was added to the mixture, and the residue was distilled with water steam. The residue was filtered with hot water, and a blue solid was dried. The compound was purified by silica gel column chromatography using hexanes/DCM (15:85, v/v) as the eluent. Evaporation of the solvent yielded a blue solid. Yield: 1.55 g (20.1%). ^{1}H NMR (500 MHz, $CDCl_3$): δ 8.15 (d, J = 4.11 Hz, 2H; α-benzo), 8.04 (dd, J = 8.01 Hz, 4H; ortho), 7.97 (d, J = 4.01 Hz, 2H; α-benzo), 7.58 (m, 4H; meta), 7.50 (m, 2H; para), 7.43 (dd, J_1 = 7.30 Hz, J_2 = 7.22 Hz, 2H; β-benzo), 7.34 (dd, J_1 = 7.13 Hz, J_2 = 7.13 Hz, 2H; β-benzo). ^{13}C NMR (125 MHz, $CDCl_3$): δ 148.6 (α-pyrrole), 143.9 (β-pyrrole), 135.4 (β-pyrrole), 133.2 (phenyl), 129.9 (β-pyrrole), 129.4 (para), 129.2 (meta), 127.7 (ortho), 127.6 (β-benzo), 126.3 (β-benzo), 122.1 (α-benzo), and 121.3 (α-benzo). UV–vis (toluene): λ_{max} = 655 nm.

Synthesis of *N*,*N*-Difluoroboryl-[*N*-(3-phenyl-2*H*-isoindol-1-yl)-*N*-(3-phenyl-1*H*-isoindol-1-ylidene)amine] (2a). Compound **2a** was prepared using a slightly modified procedure that was reported previously.[39] To a solution of the free-base aza-BODIPYH (**1**; 253 mg, 0.635 mmol) in dry toluene (35 mL) was added diisopropylethylamine (335 μL, 1.90 mmol) under an argon atmosphere, and the mixture was stirred for 15–20 min at room temperature. Then $BF_3{\cdot}OEt_2$ (470 μL, 3.81 mmol) was added to the mixture at room temperature. After 3 h of stirring, the mixture was quenched by adding 5 mL of water. After the addition of DCM, the organic layer was washed with water, dried, and evaporated under reduced pressure. The crude compound was purified by column chromatography on silica gel with CH_2Cl_2. Evaporation of the solvent yielded the metal-incorporated aza-BODIPY (aza-BODIPY/BF_2; 170 mg, 60%). ^{1}H NMR (500 MHz, $CDCl_3$): δ 8.12 (d, J = 8.05 Hz, 2H; α-benzo), 7.88 (m, 4H; ortho), 7.63 (d, J = 8.20 Hz, 2H; α-benzo), 7.53, 7.50 [m, meta (4H), para (2H), β-benzo (2H)], 7.32 (dd, J_1 = 7.45 Hz, J_2 = 7.53 Hz, 2H; β-benzo). ^{13}C NMR (125 MHz, $CDCl_3$): δ 153.5 (α-pyrrole), 140.0 (α-pyrrole), 134.0 (β-pyrrole), 131.6 (β-pyrrole), 131.0 (β-benzo), 130.7 (para), 130.5 (ortho), 128.8 (meta), 127.6 (β-benzo), 124.5 (α-benzo), 121.3 (α-benzo). UV–vis (toluene): λ_{max} = 715 nm.

Synthesis of *N*,*N*-bis(ferrocenylboroyl)[*N*-(3-phenyl-2*H*-isoindol-1-yl)-*N*-(3-phenyl-1*H*-isoindol-1-ylidene)amine] (3). Boron trichloride (1.3 equiv, 228 μL of a 1.0 M solution in hexanes) was slowly added to a solution of **1** (1.0 equiv, 70 mg, 0.17 mmol) in anhydrous toluene (20 mL) under an argon atmosphere. The reaction mixture was stirred at room temperature for 1 h. Subsequently, ethylmagnesium bromide (3 mol equiv, 0.36 mmol, 0.362 mL) was added to a solution of ethynylferrocene (3.5 equiv, 170 mg, 0.809 mmol) in anhydrous THF (5 mL). The resulting mixture was heated at 60 °C. After 2 h of refluxing, the Grignard mixture was cooled to room temperature and then transferred via a cannula to a solution mixture of aza-BODIPYH and BCl_3. The resulting mixture was stirred for 5 h. The solvent was evaporated, and the product was purified using a chromatography column packed with flash neutral alumina, using hexanes/DCM (25:75, v/v) as the eluent. Yield: 35.2 mg (21%). Elem anal. Calcd for $C_{52}H_{36}BN_3Fe_2{\cdot}0.17CH_2Cl_2{\cdot}0.16C_6H_{14}$: C, 74.79; H, 4.56; N, 4.92. Found: C, 74.79; H, 4.56; N, 4.63. ^{1}H NMR (500 MHz, $CDCl_3$): δ 8.28 (d, J = 8.40 Hz, 4H; ortho), 8.17 (d, J = 8.10 Hz, 2H; α'-benzo), 7.62 (m, 8H; α''-benzo, para, meta), 7.51 (m, 2H; β'-benzo), 7.31 (m, 2H; β''-benzo), 4.03 (5H, s, Cp), 3.98 (2H, m, α-Cp), 3.90 (2H, m, β-Cp). ^{13}C NMR (125 MHz, $CDCl_3$): δ 152.6 (α-pyrrole), 137.4 (β-pyrrole), 133.4 (β-pyrrole), 132.0 (β-pyrrole), 131.9 (para), 131.2 (β-benzo), 129.6 (ortho), 129.20 (meta), 128.3 (phenyl), 127.8 (β-benzo), 126.5 (α-benzo), 123.6 (α-benzo), 120.7 (ethynyl C), 77.4 (C_{ipso}), 71.2 (α-Cp), 69.7 (β-Cp), 68.0 (ethynyl C). UV–vis (toluene): λ_{max} = 706 nm.

X-ray Crystallography. X-ray diffraction data were collected on a Rigaku Rapid II image-plate diffractometer using graphite-monochromated Mo Kα (λ = 0.71074 Å) and Cu Kα (λ = 1.54187 Å) radiation at 123 K. Multiscan absorption corrections were applied to the data in all cases. The structures were solved by direct methods, as implemented in *SIR-92*,[55] and refined by full-matrix least squares based on F^2 using *SHELXL-2013*[56] and *SHELXLE*[57] software. Compound **1** was found to be disordered over a symmetry element (center of inversion); therefore, the occupancies for all atoms were constrained to 0.5. The geometry was restrained by using a set of geometrical restraints such as *DFIX* and *SADI*. Water molecules were found to lie on a special position (3_1) and disordered. Unfortunately, no reasonable model was obtained for the disorder. Therefore, the contribution from the disordered water molecules into the diffraction data was removed by using a *SQUEEZE* procedure, as implemented in *PLATON*.[58] All non-hydrogen atoms were refined using an anisotropic approximation, while hydrogen atoms were idealized and refined using riding mode: thermal displacement parameters for all aromatic protons were constrained to the parent atom with $U_{iso}(H) = 1.2U_{eq}(C)$, where $U_{eq} = {}^1/_3(U_{11} + U_{22} + U_{33})$. Analysis of the structures and visualization of the results were done using *PLATON* software.

Absorption, Fluorescence, Electrochemistry, and NMR. Absorption data were obtained on a Jasco 720 spectrophotometer. Electrochemical measurements were conducted using a CH Instruments electrochemical analyzer utilizing a three-electrode scheme with platinum working and auxiliary and Ag/AgCl reference electrodes in a 0.05 M solution of TBAF in DCM with redox potentials corrected using an internal standard (decamethylferrocene, Fc*) in all cases. The redox potentials were then corrected to Fc using the appropriate oxidation potentials for Fc^*/Fc^{*+} versus Fc/Fc^+ in the DCM/TBAF system. NMR spectra were recorded on a Varian INOVA instrument

DOI: 10.1021/acs.inorgchem.5b00494
Inorg. Chem. 2015, 54, 4167–4174

with a 500 MHz frequency for hydrogen and 125 MHz for carbon. Chemical shifts are reported in parts per million (ppm) and referenced to tetramethylsilane [$Si(CH_3)_4$] and deuterated chloroform ($CDCl_3$) as internal standards. In all cases, the final assignments of the ^1H and ^{13}C signals were made using COSY and HMQC spectra. Elemental analyses were conducted by Atlantic Microlab. Steady-state fluorescence data were collected using a Cary Eclipse fluorimeter at room temperature. Fluorescence quantum yields were determined against the external standard Rhodamine 800 in ethanol, which has a quantum yield of 0.19.[59]

Time-Resolved Absorption and Emission. The nanosecond to millisecond decay of **3** was measured using a flash-photolysis setup. A solution of compound **3** in toluene was placed in a 1 cm quartz cuvette. The sample was pumped using a pulsed 337 nm nitrogen laser (PTI GL-3300) with a repitition rate of 10 Hz and a fluence of 500 $\mu J/cm^2$. The optical density of the sample was 0.5 at 337 nm. The excited-state absorption of the sample was probed at a right angle to the pump with a continuous-wave 532 nm diode laser. The excited-state absorption decay was measured by detecting the probe beam using a photodiode and a digital oscilloscope.

Fluorescence lifetimes were measured using time-correlated single photon counting. Samples in a 1 cm quartz cuvette were excited with a 635 nm, 40 MHz diode laser (driver, Picoquant PDL 800-B; head, Picoquant LDH-P-635). Emission was directed through a double monochromator (Jobin-Yvon TRIAX-320) and detected using an avalanche photodiode (Picoquant MPD PDM). The instrument response of the system was approximately 500 ps full width at half-maximum (fwhm). The signal for compound **1** decayed faster than the instrument response; no signal was observed for compound **3** because of its low fluorescence quantum yield. The signal for compound **2a** is shown in Figure S8 in the Supporting Information (SI).

Transient absorption (TA) spectra were obtained using a home-built laser system consisting of a Ti:sapphire oscillator (powered by a Spectra Physics Millenia Pro) and a regenerative amplifier (powered by a Spectra Physics Empower 15). Pulse widths are controlled with a grating-based stretcher/compressor. The system gives 805 nm pulses with ~60 fs (fwhm) widths at a repetition rate of 1 kHz. Excitation pulses for TA were created by directing a portion of this light into a home-built noncollinear optical parametric amplifier (NOPA). The output of the NOPA is tunable from 480 to 700 nm with a pulse width of ~60 fs. For the experiments presented here, the NOPA was tuned to a center wavelength of 630 nm. Probe pulses for TA were created by focusing a small fraction of the 805 nm light (<1 MW) into a 2 mm sapphire window, providing a white-light continuum (420–750 nm).

Excitation polarization was kept at the magic angle (54.7°) relative to probe polarization to isolate the isotropic dynamics. The delay time between the excitation and probe pulses is controlled by a delay stage consisting of a retroreflector on a motorized stage (Newport UTM150PP.1). After the pulses were focused in the sample, the probe beam was directed through a monochromator (Princeton Instruments SP2150i) and detected using a 256 pixel diode array (Hamamatsu silicon array), giving a resolution of 2 nm/pixel. The pump beam was modulated at half the laser repetition rate, while the probe beam was measured for every laser pulse, allowing for a change in the optical density, ΔOD, induced by the pump to be calculated for each pulse pair. For each time point, 62500 pulse pairs were collected. The dependence of the ΔOD signal for pulse energies between 10 and 40 nJ was found to be linear. Data shown were collected with pulse energies of 25–35 nJ. The samples had an optical density of 0.25 and were continuously pumped through a 1 Mm flow cell during data collection to ensure a fresh sample for each laser pulse. Absorption spectra taken before and after laser illumination were indistinguishable, suggesting minimal photodegradation of the samples.

Calculations. All computations were performed using *Gaussian 09* software running under Windows or UNIX OS.[60] Molecular orbital (MO) contributions were compiled from single-point calculations using the *VMOdes* program.[61] In all calculations, the TPSSh hybrid (10% Hartree–Fock exchange)[62] exchange-correlation functional was used because it was found in a set of model gas-phase calculations that it is superior over standard generalized gradient approximation (BP86)[63] and hybrid B3LYP exchange-correlation functionals.[64,65] Indeed, the use of a hybrid B3LYP exchange-correlation functional results in the highest occupied molecular orbital (HOMO), which is a purely aza-BODIPY-centered MO in disagreement with experimental data, while that calculated using BP86 exchange-correlation functional vertical excitation energies for metal-to-ligand charge-transfer (MLCT) transitions was found to be severely underestimated. In all calculations, the 6-311G(d) basis set was employed.[66] Solvent effects were modeled using the polarizable continuum model (PCM) approach.[67] In all time-dependent density functional theory (TDDFT) calculations, the lowest 20 excited states were calculated in order to cover experimentally observed transitions in the UV–vis region.

RESULTS AND DISCUSSION

Compound **3** was prepared as outlined in Scheme 1. Organometallic **3** is a stable solid in air and can be purified by conventional chromatographic methods. However, **3** slowly degrades upon prolonged standing in solution under an ambient atmosphere. All of our attempts to prepare **4**, in which the Fc groups are directly linked to the boron atom, failed because of the steric bulk of the Fc fragment. Compound **3** was first characterized by ^1H, ^{13}C, COSY, and HMQC NMR and UV–vis spectra (Figure 1). Because of the lack of a strong

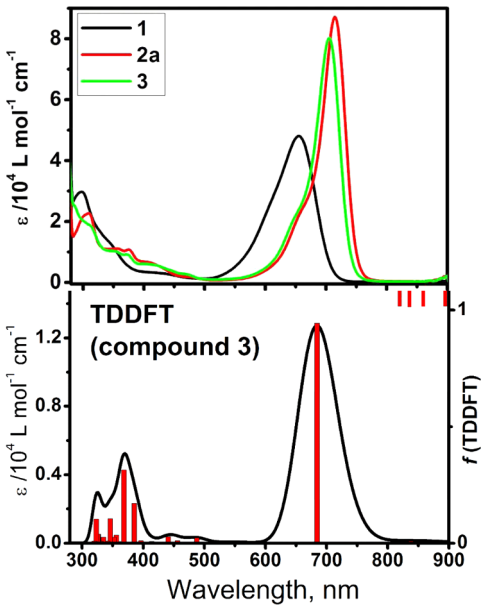

Figure 1. Experimental (top, in DCM) and PCM–TDDFT-predicted (bottom) UV–vis spectra of the target compounds. Zero-intensity low-energy MLCT bands are indicated by the vertical red bars in the upper right corner.

ring π current in **3**, the Fc group proton and carbon signals are shifted only slightly from those observed in ferrocenylacetylene. The low-energy absorption band of **2a** peaking at 715 nm is significantly shifted from that observed in the parent boron-free compound, **1**, peaking at 655 nm. Transformation of the BF_2 fragment in **2a** into $B(C{\equiv}CFc)_2$ substituents in **3** results in only a small shift in energy, with a peak absorbance at 706 nm (Figure 1).

Fluorescence. Although the absorption spectra of **2a** and **3** (Figure 1) are very similar, their fluorescence spectra and excited-state relaxation dynamics are substantially different. The steady-state emission spectra for compounds **1**–**3** are presented at the top of Figure 2. The addition of the Fc substituents

DOI: 10.1021/acs.inorgchem.5b00494
Inorg. Chem. 2015, 54, 4167–4174

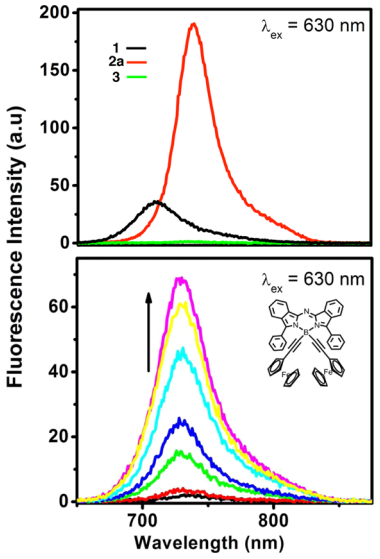

Figure 2. Steady-state fluorescence spectra in toluene (top) and fluorescence spectral change upon oxidation of **3** with $Fe(ClO_4)_3$ (bottom).

results in a dramatic loss of emission. The fluorescence quantum yield drops by over 2 orders of magnitude in **3** relative to **2a** (Table 1). Emission from **3** was recovered upon oxidation

Table 1. Absorption and Fluorescence Details for Compounds 1, 2a, and 3

compound	$\lambda_{abs,max}$ (nm)	ε (M^{-1} cm^{-1})	$\lambda_{em,max}$ (nm)	Stokes shift (nm)	Φ_{fl}
1	655	47800	709	54	0.007 ± 0.001
2a	715	87000	744	29	0.21 ± 0.03
3	706	80000	728	22	<0.001

with $Fe(ClO_4)_3$, as presented in the bottom of Figure 2. Recovery of the emission following oxidation of the Fc ligands suggests that emission quenching in the neutral molecule proceeds via charge transfer from the Fc ligand to aza-BODIPY, which is a commonly reported quenching mechanism in Fc-containing compounds.[68−74]

Electrochemistry. The redox properties of compounds **1**−**3** were studied using electrochemical cyclic voltammetry (CV) and differential-pulse voltammetry (DPV) methods, and the results are presented in Figure 3 and Table 2. In the cases of **1** and **2a**, two irreversible oxidations and one reversible and one

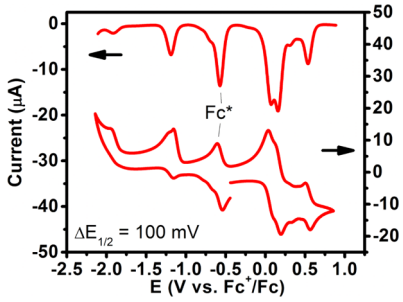

Figure 3. Room-temperature DPV (top) and CV (bottom) data on compound **3** in a DCM/0.05 M TBAF system (the internal standard decamethylferrocene is indicated as Fc*).

irreversible reductions were observed. Compound **3** shows three reversible oxidations and two irreversible reduction processes in the DCM/TBAF system.[53,54,75−78] DPV data clearly suggest that the oxidation potentials for the Fc substituents in **3** are separated by ∼100 mV, which is indicative of their electronic coupling. The computational results presented in the next section indicate that through-bond coupling between the Fc ligands and the aza-BODIPY core is weak. Although electronic coupling in boron-bridged diferrocene systems has been previously described,[79−85] the observation of electronic communication in compound **3** is surprising given the separation distance. The computational results predict through-bond (11.45 Å) and through-space (9.85 Å) Fe−Fe distances that are much longer than those in previously described systems.[86]

Calculations. The electronic structure and vertical excitation energy calculations for compounds **1**−**3** (Figures 1, 4, and S13−S18 in the SI) correlate well with the experimental results. In the case of compounds **1** and **2a**, π and π^* MOs dominate the HOMO−LUMO regions and, accordingly, their UV−vis absorption spectra can be described as consisting almost exclusively of $\pi \rightarrow \pi^*$ transitions. In agreement with the electrochemical data, there is relatively small spacing in energy between the HOMO, HOMO−1, HOMO−3, and HOMO−4 MOs in complex **3**. These orbitals are predominantly Fc-centered, while HOMO−2 is an aza-BODIPY-centered π orbital. Such an electronic structure results in the appearance of four low-energy Fc-to-aza-BODIPY MLCT transitions predicted by the TDDFT calculations (Figure 1). Taking into consideration that the (C≡CFc) substituents in **3** are not efficiently coupled to the aza-BODIPY π system, TDDFT calculations predict low intensities for such bands, in agreement with the experimental data. The most intense transition in **3** is dominated by HOMO−2-to-LUMO electron transfer and is $\pi \rightarrow \pi^*$ in its nature. In general, TDDFT calculations are in excellent agreement with the experimental UV−vis absorption data on compounds **1**−**3**.

Excited-State Dynamics. Excited-state relaxation dynamics in compounds **1**−**3** were measured using a combination of time-resolved emission and TA. TA spectra at selected time delays after excitation at 620 nm are presented in Figure 5. On the basis of the computational predictions, we assign this excitation to the $\pi \rightarrow \pi^*$ transition largely isolated on aza-BODIPY. The spectra in all cases consist of TA (positive ΔOD) at shorter wavelengths and a ground-state bleach (GB, negative ΔOD) that mirrors the static absorption spectrum at longer wavelengths. Absorption of the initially created excited state appears within the 50 fs time resolution of the experiments. The initial TA was broad and peaked at 530 nm for **1** and at ∼590 nm for **2a** and **3**. Correlated loss of the excited-state absorption and the GB in the cases of **1** and **2a** demonstrates that relaxation proceeds directly back to the ground state. The TA spectra for **1** and **2a** do not change shape with the delay time, and **1** decays 35 times faster than **2a** (Table 3). The 1.9 ns lifetime for **2a** was determined by both TA and time-correlated single photon counting (Figure S8 in the SI). A significant reduction in the measured internal conversion rate for **2a** compared to **1** is consistent with the substantial increase observed in the fluorescence quantum yield (see Table 1).

Compared with **2a**, the excited-state dynamics are more complicated for compound **3**. The shape of the TA changes on a picosecond time scale. Because the initial absorption peaking at 590 nm decays with a time constant of 1.7 ps ($k = 5.9 \times 10^{11}$

DOI: 10.1021/acs.inorgchem.5b00494
Inorg. Chem. 2015, 54, 4167−4174

Table 2. Redox Potentials (V, vs FcH/FcH$^+$) for Compounds 1, 2a, and 3 in DCM/0.05 M TBAF at Room Temperature

	oxidation			reduction	
compound	ox1	ox2	ox3	red1	red2
1		0.659 (irr)	0.175 (irr)	−1.333	−1.921 (irr)
2a		1.076 (irr)	0.558 (irr)	−1.062	−1.837 (irr)
3a	0.537	0.157	0.072	−1.190 (irr)	−1.909 (irr)

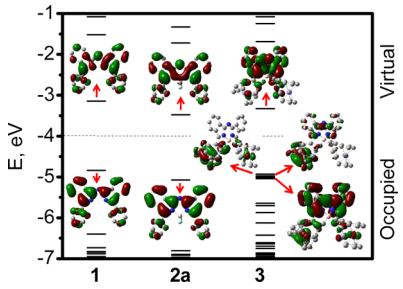

Figure 4. DFT−PCM-calculated [TPSSh/6-311G(d)] orbital energies for **1**, **2a**, and **3** with a pictorial representation of the frontier MOs.

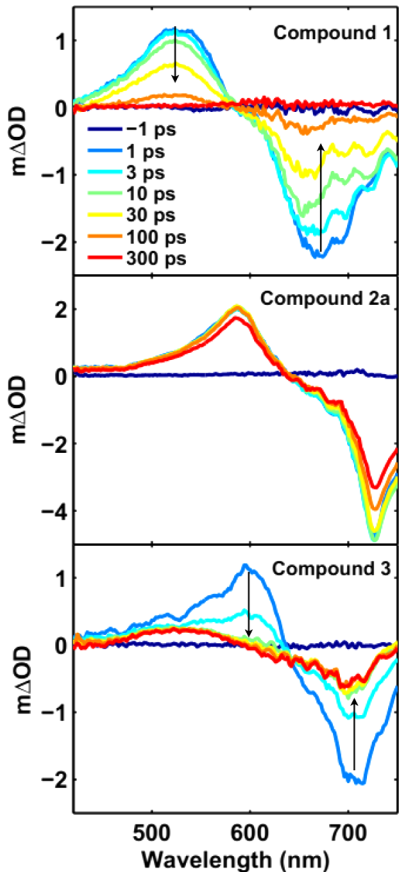

Figure 5. Time-resolved TA spectra of compounds **1**−**3** in toluene following excitation at 630 nm.

Table 3. Exicited-State Lifetimes of Compounds 1, 2a, and 3 Dissolved in Toluene

compound	τ_1 (ps)	τ_2 (μs)
1	53 ± 1	
2a	1900 ± 100	
3	1.7 ± 0.1	4.8 ± 0.1

s^{-1}; see Figure 6 and Table 3), a new absorption peaking at 520 nm appears and remains static over the experimental range of

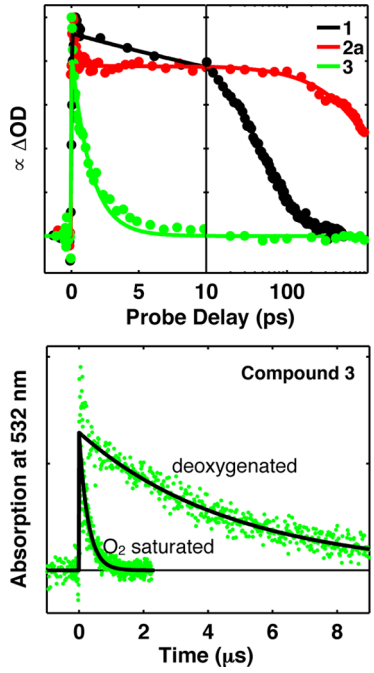

Figure 6. (top) Time dependence at the peak of TA, as shown in Figure 5. Note the broken time axis, which is linear up to 10 ps and then logarithmic. (bottom) Time-resolved TA at 532 nm of compound **3** in toluene following excitation at 308 nm. The circles are the data points, and the lines are single-exponential fits to the data. Time constants are reported in Table 1.

time delays probed in Figure 5. Rapid decay of the initial excited state and the correlated appearance of the new absorption at 520 nm indicates that the quenching mechanism is not direct internal conversion to the ground state but rather conversion to a new excited state. With a lack of evidence for intersystem crossing in the parent, **2a**, even on a nanosecond time scale, relaxation mediated by the Fc substituents must proceed by either an energy-transfer or an electron-transfer mechanism. The lack of overlap between the absorption spectrum of the Fc donor and emission spectrum of the aza-BODIPY acceptor (Figure S8 in the SI) allows us to rule out resonance energy transfer as the quenching mechanism (this is discussed quantitatively in the SI). We conclude that electron transfer is responsible for loss of the initially created excited state. According to this mechanism, electron transfer from the low-spin iron(II) center in the Fc ligand to the photoexcited aza-BODIPY π^* core is predominantly responsible for fluorescence quenching in complex **3**. In agreement with this conclusion, we have shown that stepwise oxidation of the Fc substituents by $Fe(ClO_4)_3$ results in the recovery of fluorescence (Figure 2).

DOI: 10.1021/acs.inorgchem.5b00494
Inorg. Chem. 2015, 54, 4167−4174

The same experiments were also conducted in the more polar solvent acetonitrile (Figures S10−S12 in the SI). In addition to a small shift in the absorption features to shorter wavelengths, the initial charge-separation step slows slightly to a time constant of 2.4 ± 0.2 ps. The difference in energy between the initially excited and charge-separated (CS) states of ∼0.5 eV is slightly larger than typical reorganization energies in similar systems.[87] Under these conditions, the initial charge separation is predicted to take place with a small barrier on the inverted side of Marcus theory. In the inverted regime, additional stabilization of the CS state (relative to the initial π^* state) by the more polar acetonitrile will increase the barrier and decrease the rate of charge transfer. This is illustrated in Figure 7, where the gray parabola represents additional stabilization in acetonitrile relative to the blue parabola, which represents toluene. The observed rate reduction with increasing solvent polarity supports the conclusion that charge transfer takes place in the Marcus inverted regime.

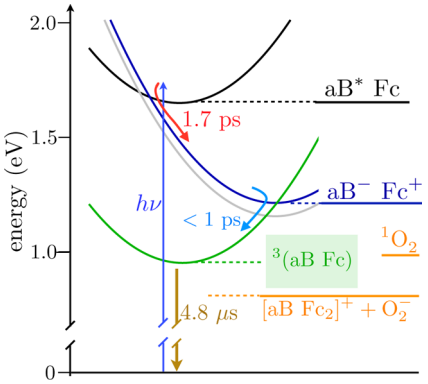

Figure 7. Energy-level diagram. "aB" is an abbreviation for aza-BODIPY.

The lifetime of the state with absorbance peaking at 520 nm was determined using flash photolysis and measuring the decay in TA at 532 nm. This is presented at the bottom of Figure 6. In the absence of molecular oxygen, the lifetime was 4.8 ± 0.1 μs in toluene. As shown in Figure 5, there is only a single transformation observed following photoexcitation, with a clean isosbestic point at 630 nm. Given the prior conclusion that deactivation is initiated by electron transfer from the Fc ligand, there are two possibilities: the long-lived state is the initially created CS state, or the CS state is converted to a subsequent state on a time scale faster than the 1.7 ps initial charge separation. The latter case has been proposed to occur in analogous systems, with rapid recombination suggested to result in the formation of a triplet state.[46] A triplet state localized on either aza-BODIPY or Fc would be located around ∼1 eV above the ground state, placing it roughly 0.3 eV below the CS state, as shown in the energy-level diagram in Figure 7.[46]

A relatively short charge-separation distance of only ∼6.5 Å between the aza-BODIPY and Fc iron centers makes a CS lifetime of >1 μs difficult to justify. In addition, there are two energetically accessible triplet states, with the triplet located on either aza-BODIPY or Fc, that allow for subsequent transformation of the CS state via charge recombination. This would have to take place more rapidly than the initial charge-separation step because no intermediate was observed in the TA measurements, placing an upper limit on the charge recombination step of ∼1 ps. An extremely rapid recombination step is consistent with the change in energy, which is very similar to typical values for the reorganization energy in analogous systems, leading to a prediction of near-barrierless transfer.[87] This is illustrated with the parabolas in Figure 7. Excess energy will also accelerate charge recombination prior to pseudoequilibration in the CS state. We conclude that the most likely identity of the long-lived excited state is a triplet state. We are not able to distinguish between the states where the triplet resides primarily on aza-BODIPY or on one of the Fc ligands.

The addition of the (C≡CFc) ligands at the boron atom leads to very rapid charge transfer and subsequent recombination in **3**. The result is efficient intersystem crossing without the inclusion of heavy atoms to enhance spin−orbit coupling. In addition to the potential advantages for optoelectronic applications that come with extending the excited-state lifetime by 3 orders of magnitude, the possibility arises of using this system as a triplet sensitizer for singlet-oxygen chemistry. When the solution was saturated with O_2, the lifetime of **3** was reduced to 0.28 ± 0.02 μs (Figure 6), indicating that the long-lived triplet state is effectively quenched by O_2. To examine the potential for sensitizing photochemical reactions, the conversion of dihydroxynapthalene to juglone in the presence of O_2 was attempted.[88] The experiments were carried out at multiple excitation wavelengths 700, 365, and 308 nm, and upon illumination with a xenon lamp. Under the same conditions where efficient conversion was observed using standard triplet sensitizers such as methylene blue, no evidence for conversion was observed when using **3** as the sensitizer. At 0.98 eV, $^1O_2$ is similar in energy to ^{3}(aza-BODIPY). The difference between the measured oxidation potential of **3** and the reduction potential for O_2 is 0.8 eV, making oxidation of the triplet the thermodynamically favored reaction, as shown in Figure 7. The absence of evidence for the production of $^1O_2$ suggests that the triplet excited state is predominantly oxidatively quenched by O_2 rather than being quenched through energy transfer.

CONCLUSION

The first aza-BODIPY complex with Fc-containing organoboron fragments was synthesized and characterized. Surprisingly, the Fc ligands in this compound are electronically coupled to each other despite unfavorable geometry, a lack of conjugation in their connectivity, and a separation distance of 10 Å. Photoinitiated charge separation takes place very rapidly and is followed by even faster charge recombination to form a triplet state in 1.7 ps in toluene. This efficient charge-transfer-mediated internal conversion results in a large increase in the excited-state lifetime from 2 ns to 4.8 μs. An energy-level diagram summarizing the excited-state dynamics is presented in Figure 7. Efficient access to the triplet state without the need to incorporate heavy atoms is not common, and in this sense, this complex does exceed the performance of other reported Fc-BODIPY conjugates, limiting the through-bond coupling between the Fc ligands and aza-BODIPY via bonding at the boron while balancing the through-space coupling with orientation and spatial proximity offers a new paradigm for tuning the electronic structures and excited-state dynamics in this class of molecules. Using charge transfer to enhance the intersystem crossing provides an additional design principle for materials targeted at optoelectronic devices.

DOI: 10.1021/acs.inorgchem.5b00494
Inorg. Chem. 2015, 54, 4167−4174

■ ASSOCIATED CONTENT

Supporting Information

X-ray crystallographic data in CIF format, X-ray, NMR, DFT data, absorption and time-resolved spectroscopy for compound **3** in acetonitrile, and a complete analysis of the potential for resonance energy transfer. This material is available free of charge via the Internet at http://pubs.acs.org.

■ AUTHOR INFORMATION

Corresponding Authors

*E-mail: blank@umn.edu.
*E-mail: vnemykin@d.umn.edu.

Author Contributions

‡E.M. and T.J.P. contributed equally to this work.

Notes

The authors declare no competing financial interest.

■ ACKNOWLEDGMENTS

This work was supported by Grants NSF CHE-1110455, NSF DMR-1006566, CHE-1401375, and NSF MRI CHE-0922366, the Minnesota Supercomputing Institute, and a University of Minnesota Grant-in-Aid to V.N.N.

■ REFERENCES

(1) Melkozernov, A. N.; Barber, J.; Blankenship, R. E. *Biochemistry* **2005**, *45*, 331−345.
(2) Guenes, S.; Neugebauer, H.; Sariciftci, N. S. *Chem. Rev.* **2007**, *107*, 1324−1338.
(3) Sun, Y.; Welch, G. C.; Leong, W. L.; Takacs, C. J.; Bazan, G. C.; Heeger, A. J. *Nat. Mater.* **2012**, *11*, 44−48.
(4) Whittell, G. R.; Hager, M. D.; Schubert, U. S.; Manners, I. *Nat. Mater.* **2011**, *10*, 176−188.
(5) El-Khouly, M. E.; Fukuzumi, S.; D'Souza, F. *ChemPhysChem* **2014**, *15*, 30−47.
(6) Karthikeyan, S.; Lee, J. Y. *J. Phys. Chem. A* **2013**, *117*, 10973−10979.
(7) Lopez-Duarte, I.; Wang, M.; Humphry-Baker, R.; Ince, M.; Martinez-Diaz, M. V.; Nazeeruddin, M. K.; Torres, T.; Graetzel, M. *Angew. Chem., Int. Ed.* **2012**, *51*, 1895−1898.
(8) Ma, R.; Guo, P.; Yang, L.; Guo, L.; Zhang, X.; Nazeeruddin, M. K.; Graetzel, M. *J. Phys. Chem. A* **2010**, *114*, 1973−1979.
(9) Ragoussi, M. E.; Ince, M.; Torres, T. *Eur. J. Org. Chem.* **2013**, *2013*, 6475−6489.
(10) Sharma, G. D.; Daphnomili, D.; Gupta, K. S. V.; Gayathri, T.; Singh, S. P.; Angaridis, P. A.; Kitsopoulos, T. N.; Tasis, D.; Coutsolelos, A. G. *RSC Adv.* **2013**, *3*, 22412−22420.
(11) Wu, C.-H.; Chen, M.-C.; Su, P.-C.; Kuo, H.-H.; Wang, C.-L.; Lu, C.-Y.; Tsai, C.-H.; Wu, C.-C.; Lin, C.-Y. *J. Mater. Chem. A* **2014**, *2*, 991−999.
(12) An, M.; Kim, S.; Hong, J.-D. *Bull. Korean Chem. Soc.* **2010**, *31*, 3272−3278.
(13) Dammer, S. J.; Solntsev, P. V.; Sabin, J. R.; Nemykin, V. N. *Inorg. Chem.* **2013**, *52*, 9496−9510.
(14) González-Cabello, A.; Vázquez, P.; Torres, T. *J. Organomet. Chem.* **2001**, *637*−*639*, 751−756.
(15) Gonzalez-Cabello, A.; Claessens, C. G.; Martin-Fuch, G.; Ledoux-Rack, I.; Vazquez, P.; Zyss, J.; Agulló-López, F.; Torres, T. *Synth. Met.* **2003**, *137*, 1487−1488.
(16) Gryko, D. T.; Piechowska, J.; Jaworski, J. S.; Gałezowski, M.; Tasior, M.; Cembor, M.; Butenschön, H. *New J. Chem.* **2007**, *31*, 1613−1619.
(17) Jin, Z.; Nolan, K.; Mcarthur, C. R.; Lever, A. B. P.; Leznoff, C. C. *J. Organomet. Chem.* **1994**, *468*, 205−212.
(18) Kubo, M.; Mori, Y.; Otani, M.; Murakami, M.; Ishibashi, Y.; Yasuda, M.; Hosomizu, K.; Miyasaka, H.; Imahori, H.; Nakashima, S. *J. Phys. Chem. A* **2007**, *111*, 5136−5143.
(19) Lukyanets, E. A.; Nemykin, V. N. *J. Porphyrins Phthalocyanines* **2010**, *14*, 1−40.
(20) Maiya, G. B.; Barbe, J. M.; Kadish, K. M. *Inorg. Chem.* **1989**, *28*, 2524−2527.
(21) Nemykin, V. N.; Kobayashi, N. *Chem. Commun.* **2001**, *0*, 165−166.
(22) Nemykin, V. N.; Barrett, C. D.; Hadt, R. G.; Subbotin, R. I.; Maximov, A. Y.; Polshin, E. V.; Koposov, A. Y. *Dalton Trans.* **2007**, 3378−3389.
(23) Nemykin, V. N.; Galloni, P.; Floris, B.; Barrett, C. D.; Hadt, R. G.; Subbotin, R. I.; Marrani, A. G.; Zanoni, R.; Loim, N. M. *Dalton Trans.* **2008**, 4233−4246.
(24) Nemykin, V. N.; Purchel, A. A.; Spaeth, A. D.; Barybin, M. V. *Inorg. Chem.* **2013**, *52*, 11004−11012.
(25) Poon, K. W.; Yan, Y.; Li, X. Y.; Ng, D. *Organometallics* **1999**, *18*, 3528−3533.
(26) Rohde, G. T.; Sabin, J. R.; Barrett, C. D.; Nemykin, V. N. *New J. Chem.* **2011**, *35*, 1440−1448.
(27) Shoji, O.; Tanaka, H.; Kawai, T.; Kobuke, Y. *J. Am. Chem. Soc.* **2005**, *127*, 8598−8599.
(28) Solntsev, P. V.; Sabin, J. R.; Dammer, S. J.; Gerasimchuk, N. N.; Nemykin, V. N. *Chem. Commun.* **2010**, *46*, 6581−6583.
(29) Sugimoto, H.; Tanaka, T.; Osuka, A. *Chem. Lett.* **2011**, *40*, 629−631.
(30) Suijkerbuijk, B. M. J. M.; Klein Gebbink, R. J. M. *Angew. Chem., Int. Ed.* **2008**, *47*, 7396−7421.
(31) Vecchi, A.; Galloni, P.; Floris, B.; Nemykin, V. N. *J. Porphyrins Phthalocyanines* **2013**, *17*, 165−196.
(32) Venkatraman, S.; Kumar, R.; Sankar, J.; Chandrashekar, T. K.; Sendhil, K.; Vijayan, C.; Kelling, A.; Senge, M. O. *Chem.—Eur. J.* **2004**, *10*, 1423−1432.
(33) Xu, Q. Y.; Barbe, J. M.; Kadish, K. M. *Inorg. Chem.* **1988**, *27*, 2373−2378.
(34) Baudron, S. A. *Dalton Trans.* **2013**, *42*, 7498−7509.
(35) Benniston, A. C.; Copley, G. *Phys. Chem. Chem. Phys.* **2009**, *11*, 4124−4131.
(36) Boens, N.; Leen, V.; Dehaen, W. *Chem. Soc. Rev.* **2012**, *41*, 1130−1172.
(37) Bura, T.; Hablot, D.; Ziessel, R. *Tetrahedron Lett.* **2011**, *52*, 2370−2374.
(38) Culzoni, M. J.; Munoz de la Pena, A.; Machuca, A.; Goicoechea, H. C.; Babiano, R. *Anal. Methods* **2013**, *5*, 30−49.
(39) Donyagina, V. F.; Shimizu, S.; Kobayashi, N.; Lukyanets, E. A. *Tetrahedron Lett.* **2008**, *49*, 6152−6154.
(40) Gryko, D. T.; Gryko, D.; Lee, C.-H. *Chem. Soc. Rev.* **2012**, *41*, 3780−3789.
(41) Loudet, A.; Burgess, K. *Chem. Rev.* **2007**, *107*, 4891−4932.
(42) Min, J.; Ameri, T.; Gresser, R.; Lorenz-Rothe, M.; Baran, D.; Troeger, A.; Sgobba, V.; Leo, K.; Riede, M.; Guldi, D. M.; Brabec, C. J. *ACS Appl. Mater. Interfaces* **2013**, *5*, 5609−5616.
(43) Shi, W.-J.; Menting, R.; Ermilov, E. A.; Lo, P.-C.; Roeder, B.; Ng, D. K. P. *Chem. Commun.* **2013**, *49*, 5277−5279.
(44) Ulrich, G.; Ziessel, R.; Harriman, A. *Angew. Chem., Int. Ed.* **2008**, *47*, 1184−1201.
(45) Ziessel, R.; Ulrich, G.; Harriman, A. *New J. Chem.* **2007**, *31*, 496−501.
(46) Amin, A. N.; El-Khouly, M. E.; Subbaiyan, N. K.; Zandler, M. E.; Supur, M.; Fukuzumi, S.; D'Souza, F. *J. Phys. Chem. A* **2011**, *115*, 9810−9819.
(47) Bandi, V.; El-Khouly, M. E.; Ohkubo, K.; Nesterov, V. N.; Zandler, M. E.; Fukuzumi, S.; D'Souza, F. *Chem.—Eur. J.* **2013**, *19*, 7221−7230.
(48) Dhokale, B.; Gautam, P.; Mobin, S. M.; Misra, R. *Dalton Trans.* **2013**, *42*, 1512−1518.
(49) Galangau, O.; Fabre-Francke, I.; Munteanu, S.; Dumas-Verdes, C.; Clavier, G.; Meallet-Renault, R.; Pansu, R. B.; Hartl, F.; Miomandre, F. *Electrochim. Acta* **2013**, *87*, 809−815.
(50) Khan, T. K.; Pissurlenkar, R. R. S.; Shaikh, M. S.; Ravikanth, M. *J. Organomet. Chem.* **2012**, *697*, 65−73.

DOI: 10.1021/acs.inorgchem.5b00494
Inorg. Chem. 2015, 54, 4167−4174

(51) Liu, J.-Y.; El-Khouly, M. E.; Fukuzumi, S.; Ng, D. K. P. *ChemPhysChem* **2012**, *13*, 2030−2036.
(52) Misra, R.; Dhokale, B.; Jadhav, T.; Mobin, S. M. *Dalton Trans.* **2013**, *42*, 13658−13666.
(53) Barriere, F.; Geiger, W. E. *J. Am. Chem. Soc.* **2006**, *128*, 3980−3989.
(54) Geiger, W. E.; Connelly, N. G. *Adv. Organomet. Chem.* **1985**, *24*, 87−130.
(55) Altomare, A.; Cascarano, G.; Giacovazzo, G.; Guagliardi, A.; Burla, M. C.; Polidori, G.; Camalli, M. *J. Appl. Crystallogr.* **1994**, *27*, 435−435.
(56) Sheldrick, G. M. *Acta Crystallogr., Sect. A* **2008**, *64*, 112−122.
(57) Huebschle, C. B.; Sheldrick, G. M.; Dittrich, B. *J. Appl. Crystallogr.* **2011**, *44*, 1281−1284.
(58) Spek, A. L. *Acta Crystallogr.* **2009**, *65*, 148−155.
(59) Sauer, M.; Han, K. T.; Müller, R.; Nord, S.; Schulz, A.; Seeger, S.; Wolfrum, J.; Arden-Jacob, J.; Deltau, G.; Marx, N. J.; Zander, C.; Drexhage, K. H. *J. Fluoresc.* **1995**, *5*, 247−261.
(60) Frisch, M. J. et al. *Gaussian 03*, revision C.02; Gaussian, Inc.: Wallingford, CT, 2004.
(61) Nemykin, V., Basu, P. *VMOdes Program*, revision A; University of Minnesota—Duluth: Duluth, MN, 2001, 2003, 2005.
(62) Tao, J.; Perdew, J. P.; Staroverov, V. N.; Scuseria, G. E. *Phys. Rev. Lett.* **2003**, *91*, 146401.
(63) Becke, A. D. *Phys. Rev. A* **1988**, *38*, 3098−3100.
(64) Becke, A. D. *J. Chem. Phys.* **1993**, *98*, 1372−1377.
(65) Lee, C. T.; Yang, W. T.; Parr, R. G. *Phys. Rev. B* **1988**, *37*, 785−789.
(66) McLean, A. D.; Chandler, G. S. *J. Chem. Phys.* **1980**, *72*, 5639−5648.
(67) Scalmani, G.; Frisch, M. J.; Mennucci, B.; Tomasi, J.; Cammi, R.; Barone, V. *J. Chem. Phys.*. **2006***124*.
(68) Chen, S.; Chen, W.; Shi, W.; Ma, H. *Chem.—Eur. J.* **2012**, *18*, 925−930.
(69) Honda, T.; Nakanishi, T.; Ohkubo, K.; Kojima, T.; Fukuzumi, S. *J. Am. Chem. Soc.* **2010**, *132*, 10155−10163.
(70) Natali, M.; Ravaglia, M.; Scandola, F.; Boixel, J.; Pellegrin, Y.; Blart, E.; Odobel, F. *J. Phys. Chem. C* **2013**, 130912075807001.
(71) Oton, F.; del Carmen Gonzalez, M.; Espinosa, A.; Ramirez de Arellano, C.; Tarraga, A.; Molina, P. *J. Org. Chem.* **2012**, *77*, 10083−10092.
(72) Rochford, J.; Rooney, A. D.; Pryce, M. T. *Inorg. Chem.* **2007**, *46*, 7247−7249.
(73) Stalin Elanchezhian, V.; Kandaswamy, M. *Inorg. Chem. Commun.* **2010**, *13*, 1109−1113.
(74) Zhuo, Y.; Han, J.; Tang, L.; Liao, N.; Gui, G.-F.; Chai, Y.-Q.; Yuan, R. *Sens. Actuators, B* **2014**, *192*, 791−795.
(75) Goetsch, W. R.; Solntsev, P. V.; Van Stappen, C.; Purchel, A. A.; Dudkin, S. V.; Nemykin, V. N. *Organometallics* **2014**, *33*, 145−157.
(76) Hildebrandt, A.; Schaarschmidt, D.; Lang, H. *Organometallics* **2011**, *30*, 556−563.
(77) Hildebrandt, A.; Lehrich, S. W.; Schaarschmidt, D.; Jaeschke, R.; Schreiter, K.; Spange, S.; Lang, H. *Eur. J. Inorg. Chem.* **2012**, *2012*, 1114−1121.
(78) Solntsev, P. V.; Dudkin, S. V.; Sabin, J. R.; Nemykin, V. N. *Organometallics* **2011**, *30*, 3037−3046.
(79) Cowan, D. O.; Shu, P.; Hedberg, F. L.; Rossi, M.; Kistenmacher, T. J. *J. Am. Chem. Soc.* **1979**, *101*, 1304−1306.
(80) Heilmann, J. B.; Qin, Y.; Jaekle, F.; Lerner, H.-W.; Wagner, M. *Inorg. Chim. Acta* **2006**, *359*, 4802−4806.
(81) Kaufmann, L.; Breunig, J.-M.; Vitze, H.; Schoedel, F.; Nowik, I.; Pichlmaier, M.; Bolte, M.; Lerner, H.-W.; Winter, R. F.; Herber, R. H.; Wagner, M. *Dalton Trans.* **2009**, 2940−2950.
(82) Scheibitz, M.; Heilmann, J. B.; Winter, R. F.; Bolte, M.; Bats, J. W.; Wagner, M. *Dalton Trans.* **2005**, 159−170.
(83) Tahara, K.; Akita, T.; Katao, S.; Kikuchi, J. *Dalton Trans.* **2014**, *43*, 1368−1379.
(84) Venkatasubbaiah, K.; Pakkirisamy, T.; Lalancette, R. A.; Jaekle, F. *Dalton Trans.* **2008**, 4507−4513.
(85) Venkatasubbaiah, K.; Doshi, A.; Nowik, I.; Herber, R. H.; Rheingold, A. L.; Jaekle, F. *Chem.—Eur. J.* **2008**, *14*, 444−458.
(86) Ziegler, C. J.; Chanawanno, K.; Hasheminsasab, A.; Zatsikha, Y. V.; Maligaspe, E.; Nemykin, V. N. *Inorg. Chem.* **2014**, *53*, 4751−4755.
(87) Jin, J. L.; Wu, S. X.; Geng, Y.; Yang, S. Y. *Int. J. Quantum Chem.* **2012**, submitted.
(88) Guo, S.; Ma, L.; Zhao, J.; Küçüköz, B.; Karatay, A.; Hayvali, M.; Yaglioglu, H. G.; Elmali, A. *Chem. Sci.* **2013**, *5*, 489−500.

DOI: 10.1021/acs.inorgchem.5b00494
Inorg. Chem. 2015, 54, 4167−4174